

# 5

# Interatomic potentials

Calculating the properties of a solid based on atoms requires a description of the energetics and forces between those atoms. This energy could be calculated by solving the quantum mechanics of all the nuclei and electrons in a system, as discussed in Chapter 4. In this chapter, however, we discuss a less computationally intensive approach, in which we develop and use models for the interactions between atoms, which are generally based on simple functional forms that reflect the various types of bonding seen in solids. We shall see that these functions are, by their nature, approximate, and thus the calculations based on them are also approximations of the materials they are designed to describe. However, the use of these potentials, though lower fidelity, will enable us to model much larger systems over much larger times than possible with the more accurate quantum mechanical methods.

## 5.1 THE COHESIVE ENERGY

The goal of most atomistic-level simulations is, in part, to calculate quantities that define the energetics and thermodynamics of materials. The most fundamental of those quantities is the potential energy, which is the sum of the energetic interactions between the atoms. At 0 K, that energy is the cohesive energy, which is defined as the energy required to assemble a solid from its constituent atoms and molecules.

Consider a system of  $N$  atoms. The cohesive energy,  $U$ , is the negative of the energy needed to take all the atoms and move them infinitely far apart, i.e.,

$$U = E(\text{all atoms}) - \sum_{i=1}^N E_i , \quad (5.1)$$

where  $E(\text{all atoms})$  is the total energy of the system and  $E_i$  is the energy of an individual isolated atom.

Our goal is to develop simple analytical potentials that *approximate* the interaction energies between atoms.<sup>1</sup> The fundamental entities are the atoms and molecules that make up the solid, with the details of the electrons and nuclear charges being approximated in the analytical potentials. Thus, the simple potential functions are, in some sense, an average over the electrons and represent a great simplification over having to deal with the electrons individually. The

<sup>1</sup> Intermolecular interactions are covered in Chapter 8.

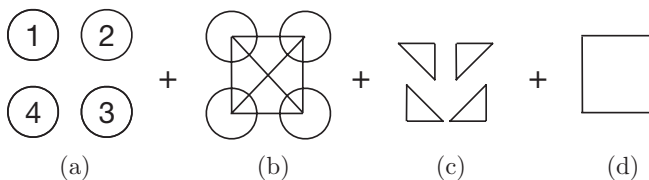


**Figure 5.1** Hierarchy of interactions between atoms: pair interactions.

procedure of developing models at one scale by averaging over properties at a lower scale is a theme in materials modeling, and will be revisited in later chapters.

The cohesive energy  $U$  in Eq. (5.1) can be formally expanded in a series of terms that depend on the individual atoms, pairs of atoms, triplets of atoms, etc., as in

$$U = \sum_{i=1}^N v_1(\mathbf{r}_i) + \frac{1}{2} \sum_{i=1}^N \sum_{j=1}' \phi_{ij}(\mathbf{r}_i, \mathbf{r}_j) + \frac{1}{6} \sum_{i=1}^N \sum_{j=1}^N \sum_{k=1}' v_3(\mathbf{r}_i, \mathbf{r}_j, \mathbf{r}_k) + \dots, \quad (5.2)$$

where the ' indicates that the  $i = j$  terms and the  $i = j = k$  terms are not included in the second and third sets of sums, respectively. This expression is shown schematically for a system of  $N = 4$  atoms in Figure 5.1:

- (a) Figure 5.1a shows the four atoms of the system. The first term in Eq. (5.2),  $v_1$ , represents the effect of an external field (for example, an electric, magnetic, or gravitational field) on the atoms. We will generally not need to be concerned with this term in this text.
- (b) Figure 5.1b represents a sum over the interaction of all pairs of atoms, as indicated in Figure 5.1b.  $\phi_{ij}(\mathbf{r}_i, \mathbf{r}_j)$  is a function of the atomic positions that represents the interaction between the pair of atoms ( $i, j$ ), located at  $\mathbf{r}_i$  and  $\mathbf{r}_j$ , respectively. Most of our discussion will center on these types of interaction.  $\phi_{ij}(\mathbf{r}_i, \mathbf{r}_j)$  is called a *pair potential* and, since it is an energy,  $\phi_{ij} = \phi_{ji}$ .
- (c) Figure 5.1c arises from the interaction of triplets of atoms,  $v_3(\mathbf{r}_i, \mathbf{r}_j, \mathbf{r}_k)$ . These types of interactions are called *three-body* interactions. Any interactions that involve more than two atoms at a time are called *many-body* interactions. While pair potentials are adequate to describe many materials, there are important classes of materials whose interaction potentials involve many-body terms, e.g., metals, covalent solids, etc., as shall be discussed later in this chapter.
- (d) Figure 5.1d is representative of a four-body interaction, i.e.,  $v_4(\mathbf{r}_1, \mathbf{r}_2, \mathbf{r}_3, \mathbf{r}_4)$ . If there were more than four atoms in this example, evaluating the contributions of these terms to the energy would consist of sums over four quartets of atoms.

## 5.2 INTERATOMIC POTENTIALS

Interatomic potentials are the potentials between atoms – we are leaving molecular systems to a later chapter. The potential forms we will discuss should reflect the *bonding* between the atoms. In Figure 5.2 we show a schematic view of the bonding in simple types of solids. The simplest bonding occurs in rare-gas solids (He, Ne, Ar, Kr, Xe) as shown in Figure 5.2a,

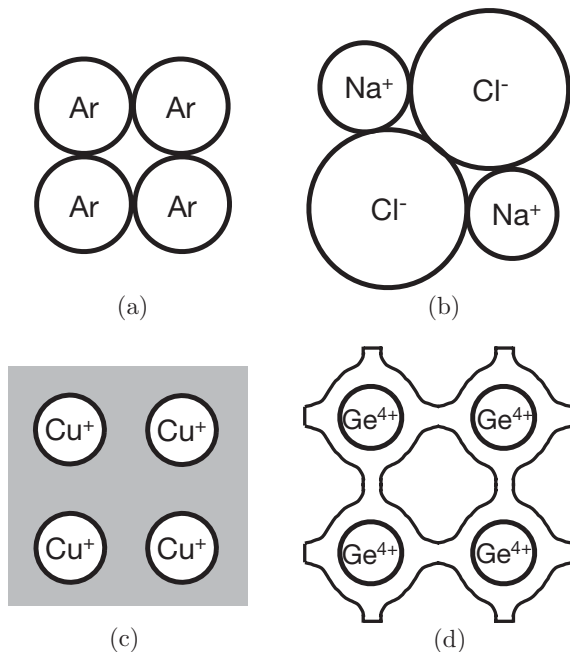


**Figure 5.2** Schematic view of bonding in atomic solids. The sizes of the atoms and ions are roughly equal to the appropriate atomic or ionic radii. Adapted from [15]. (a) Rare-gas solids. The inner core electrons and nucleus are surrounded by a closed shell of valence electrons. (b) Ionic solids. The inner core electrons and nucleus are surrounded by a closed shell of valence electrons. Note the difference in size between the cation (positive charge) and anion (negative charge). (c) Metals. The inner core electrons and nucleus form a positive ion, which is surrounded by a gas of electrons. (d) Covalent solids. The atoms have an ionic core with strong directional bonds that connect the atoms.

which are all closed-shell atoms. There is essentially no directionality to the bonds and, thus, the interatomic potentials depend entirely on the distance between the atoms. In Figure 5.2b we show a prototypical ionic material,  $\text{Na}^+\text{Cl}^-$ . Again, the atoms are closed shell and thus the bonding is essentially non-directional. Metals (Figure 5.2c) have very different electronic structures. The atoms are ionized (e.g.,  $\text{Cu}^+$  in the figure), with the valance electrons distributed throughout the system. In simple metals there is again no (or very little) directionality to the bonds, but the interaction between the delocalized electrons must be included in the description of the bonding. Finally, in Figure 5.2d we have a covalent crystal, with strong directional bonds connecting the atoms. In all cases, accurate descriptions of the interatomic potentials must reflect the nature of the electronic structure and, thus, the interactions. Of course, in real systems it is not so simple. Most systems are not strictly one type or another – they may be metals with some covalency, or partially ionic covalent crystals. In these cases, the simple models discussed in this text may need to be modified.

### 5.2.1 Basic forms of interatomic interactions

Before discussing models for interatomic interactions, a few words about the origins of the interactions are in order. For now, we will restrict the discussion to neutral atoms with non-bonding interactions. Extensions to ionic and covalently bonded systems will be discussed later in the chapter.

Suppose we have two atoms,  $i$  and  $j$ , located at  $\mathbf{r}_i$  and  $\mathbf{r}_j$ , respectively. The *interaction energy* between the two atoms is defined as the difference in energy between the energy of the pair of atoms,  $E(i + j)$ , and the energies of the individual atoms,  $E(i)$  and  $E(j)$ , separated at infinity:

$\phi_{ij}(\mathbf{r}_i, \mathbf{r}_j) = E(i + j) - E(i) - E(j)$ . We know, based on simple reasoning, something about the form of  $\phi_{ij}$ . If the separation between the atoms,  $r_{ij} = |\mathbf{r}_j - \mathbf{r}_i|$ , is sufficiently small, then the atoms must repel each other or matter would collapse. For larger separations, however, there must be a net attractive interaction between atoms or matter would not form solids and fluids at normal pressures.

### Interactions at short range

There are a number of ways that we can understand the repulsive nature of short-range interactions. Suppose we have two neutral atoms being brought together. Each atom consists of a positively charged nucleus and a distribution of electrons. When the atoms are far enough apart that there is no overlap of the charge distributions, the net electrostatic interaction is zero, since the atoms are neutral. Once the atoms are close enough so that their charge distributions overlap, increasing the Coulomb repulsion between the ions.

The electrostatic interaction is not, however, the only origin of the repulsive interactions between atoms. There is a quantum mechanical effect that arises when the charge distributions overlap and the electrons are forced to occupy a smaller volume. From the discussion of the particle in a box in Appendix F.5.1, the energy scales as  $L^{-2}$ , where  $L$  is the linear region in which the electrons are confined. As the volume in which the electrons are constrained decreases, the energy increases, leading to a repulsive interaction between the atoms. Since this effect arises from the need to maintain orthogonal wave functions (as in the particle in a box) and since only two electrons can be in an energy state, it is an example of the Pauli exclusion principle.

The density of electrons around an atom decreases exponentially with distance. The short-range interactions can be modeled with the general form

$$\phi_{SR}(r) = Ae^{-\alpha r}. \quad (5.3)$$

This energy represents a *repulsive* contribution to the energy, i.e., as the atoms are brought together the energy increases – there is a repulsive force between them.

### Nonbonding, nonionic interactions at long range

The analysis just given describes the interactions at short range, when the electronic distributions of the interacting atoms overlap. There are important interactions between atoms separated by distances long compared to the size of their electronic distributions, with the result that there is an additional attractive term that must be added to the short-range repulsive term described above. It arises from the fluctuations of the electronic clouds and is called the *dispersion energy*. It is also often referred to as the *van der Waals* energy, after the great Dutch physicist.

The *Drude* model for dispersion (van der Waals) forces is based on a model by London and described in detail in [146]. Other, more formal, methods for deriving these forces are discussed in many other places, including [159].

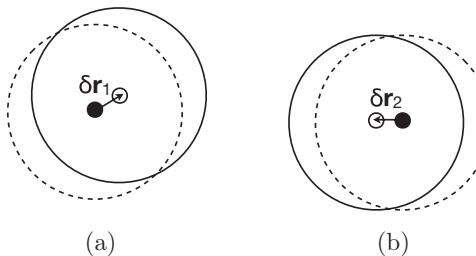


**Figure 5.3** A schematic view of dispersion interactions. The nuclei are shown as small filled circles surrounded by dashed circles that indicate the equilibrium distribution of valence electrons. The large solid circles represent the valence electron cloud centered (small open circles) a distance  $\delta\mathbf{r}$  away from the nucleus.

Electrons in an atom are not static – they fluctuate around their nucleus, destroying the spherical symmetry. These fluctuations can create a situation in which there may be more electrons on one side of the nucleus than the other, i.e., the fluctuations create an instantaneous dipole moment on the atom.<sup>2</sup> In Figure 5.3 we show a highly schematic representation of such fluctuations in which the nuclei are shown as small filled circles surrounded by dashed circles that indicate the equilibrium distribution of the valence electrons, where for simplicity we assume that all  $N$  valence electrons are located in a spherical shell (with charge  $-N$ ) centered on the nucleus (with charge  $N$ ).<sup>3</sup> If the valence electrons move, either by a fluctuation or induced by an external field, their center of charge moves to the small open circles, located  $\delta\mathbf{r}$  away from the nucleus. The sphere of charge of the moved electron shell is shown as the solid large circles.

There must be, of course, a restoring force that binds the electrons to their nucleus. Since the fluctuations are small, a harmonic binding force can be used, with energy  $1/2 k\delta\mathbf{r}^2$ . The force constant is  $k = N^2/\alpha$ , where  $N$  is the number of valence electrons and  $\alpha$  is the polarizability of the atom.  $\alpha$  is a measure of the tendency of a charge distribution to be distorted from its normal shape by an external electric field.<sup>4</sup> There is a quantum zero-point energy associated with the harmonic motion, with a value for an isolated atom of  $3\hbar\omega/2$ , where  $\omega = \sqrt{k/m}$  and  $m$  is the effective mass of the electrons.<sup>5</sup>

With two interacting atoms, the energy includes the zero-point motions of the shells as well as the electrostatic interactions. With no fluctuations, the electrostatic interactions would be zero – the net charge on each atom is 0.<sup>6</sup> When fluctuating, the instantaneous dipole on one atom interacts with the instantaneous dipole on the other. These dipole-dipole interactions change the motion of the fluctuating charges, leading to a change in the frequency of the fluctuations. This change in frequency leads to a change in the zero-point energy of the fluctuations, thus

<sup>2</sup> For a discussion of the electrostatic moments, please see Appendix E.3.

<sup>3</sup> The core electrons are assumed to be so tightly bound to the nucleus that their fluctuations are negligible.

<sup>4</sup> Suppose the atom is put in an external electric field  $\mathbf{E}$ . The outer shell containing  $N$  electrons will be shifted from the nucleus by some displacement  $\delta\mathbf{r}$ . If the shell is bound by a harmonic force, then the restoring force would be  $-k\delta\mathbf{r}$ , which must equal the total electrostatic force of  $-N\mathbf{E}$  (force equals charge times field). Thus,  $k\delta\mathbf{r} = -N\mathbf{E}$  or  $\delta\mathbf{r} = -(N/k)\mathbf{E}$ . This displacement produces a dipole moment (Eq. (E.13)) of  $\mu = -N\delta\mathbf{r} = (N^2/k)\mathbf{E}$ , which, from the definition of the polarizability  $\alpha$ , allows us to associate  $\alpha = N^2/k$ .

<sup>5</sup> From Eq. (F.26) the energy for a one-dimensional harmonic oscillator in the ground state ( $n = 0$ ) is  $\hbar\omega/2$ . In three dimensions, there would be harmonic degrees of freedom in each direction, each with a contribution of  $\hbar\omega/2$  to the zero-point energy.

<sup>6</sup> Assuming neutral atoms. Additional energetic terms from induced moments arise when ions are involved.

making a contribution to the interatomic interaction potential. Without presenting the formal derivation,<sup>7</sup> we find that for interacting, non-ionic, closed-shell systems, the leading term of the long-range attraction goes as

$$\phi_{vdw}(r) = -\frac{A}{r^6}, \quad (5.4)$$

where  $A$  is some material-dependent constant.

$\phi_{vdw}$  in Eq. (5.4) goes by a number of names, as mentioned above. For this text, we will generally refer to it as the van der Waals energy. These interactions are very weak relative to other types of bonding. They are, however, extremely important for many systems, especially molecular systems, for which they often provide much of the binding energy.

### 5.2.2 A note on units

In Appendix A.2 we discuss various energy units and how one can convert between them. Units used to describe interatomic potentials depend in large part on the types of bonding the potentials are describing. For closed-shell rare-gas atoms, in which the energies are small, it is not uncommon to use Kelvin (K) to describe the energies, though you will also see erg, joules, and electron volt (eV) used. For metals, electron volts are the most common unit. Chemical units, such as kcal/mol or kJ/mol, are also sometimes used. The important thing is to be able to convert from whatever unit in which a potential is reported to one that is consistent with how you want to use it.

## 5.3 PAIR POTENTIALS

The potential functions that we describe next are models – approximations to the real interactions. They will generally be empirical, with parameters that must be determined in some way. In the end, the models may not even be particularly accurate. Thus, when one examines any calculations based on approximate potentials, it is good to treat them with at least some skepticism. So why study these functions? We will see that even when these potential functions are not particularly good representations of the real interactions between atoms, calculations based on them can shed light on important materials processes, providing understanding of materials structure and behavior not possible otherwise.

### 5.3.1 The Lennard-Jones potential

The Lennard-Jones (LJ) potential is commonly used because it is simple and yet provides a good description of central-force interatomic interactions [161]. While it was developed to describe the general interaction between closed-shell atoms and molecules, the Lennard-Jones potential has been used to model almost everything.

<sup>7</sup> For a more detailed derivation, see [146, 170].

## Constructing the Lennard-Jones model

The Lennard-Jones potential provides a good example of the procedure for model building described in Section 1.4:

- (a) Following Figure 1.2, we first need to define the input and output. Our goal is to create a potential that will describe the interaction energy  $\phi(r)$  (the output) between two spherical atoms and thus will depend (except for materials-specific parameters) only on the distance  $r$  between them (the input).
- (b) To create the model, the physical mechanisms that govern how the molecules interact with each other must be identified. We have discussed that at short range there must be a repulsive interaction between the atoms. At longer range, since matter is bound, there must be some sort of attractive interaction.
- (c) Our goal is to find a generic form for a potential that can be applied at least *semi-quantitatively* to many materials. This requirement defines in an approximate way both how accurate the model must be and how its quality as a model can be assessed by comparing predictions based on the model to experimental data.
- (d) We have already seen in Eq. (5.4) that for interacting, non-ionic, closed-shell systems, the leading term of the long-range attraction goes as  $-1/r^6$ . The long-range form of the potential is thus assumed to take the form  $-A/r^6$ , where  $A$  is a constant that depends on the types of interacting atoms. When developed by Lennard-Jones, the form of the short-range repulsion was not known, though he assumed that it should dominate the attractive part at short range and decay with  $r$  faster than  $r^{-6}$  at long range. Strictly for convenience, the short-range interaction was assumed to take the form  $B/r^{12}$ , where  $B$  is again some constant specific to the types of interacting atoms. The short-range term mimics the exponential form discussed in Eq. (5.3). We will compare the two forms in Figure 5.6b. The choice for an exponent of 12 is rather arbitrary, but it leads to a very simple expression that is computationally convenient. The net potential has the form

$$\phi(r) = \frac{B}{r^{12}} - \frac{A}{r^6}, \quad (5.5)$$

the input is  $r$  and the output is  $\phi$ .

- (e) Since the goal is to have a potential that is generic and easy to use, the Lennard-Jones potential is usually rewritten into a dimensionally more useful form that depends on two different parameters:  $\sigma$ , which is the distance at which the potential is zero,  $\phi(\sigma) = 0$ , and  $\epsilon$ , the absolute value of the minimum of the potential. With these parameters, the Lennard-Jones potential takes the form

$$\phi(r) = 4\epsilon \left( \left( \frac{\sigma}{r} \right)^{12} - \left( \frac{\sigma}{r} \right)^6 \right). \quad (5.6)$$

The parameter sets are related by  $\sigma = (B/A)^{1/6}$  and  $\epsilon = A^2/4B$ .

- (f) In this and later chapters we will implement the Lennard-Jones potential into codes and use it to simulate various properties of materials. We will also examine how well the potential actually models real materials and will suggest improvements.

The Lennard-Jones potential is easy to characterize. For example, the point where the potential is zero is  $r = \sigma$ , i.e.,  $\phi(\sigma) = 0$ . The position of the potential minimum  $r_m$  is found by solving for the value of  $r$  such that  $d\phi/dr = 0$ . The minimum is characterized by  $r_m = 2^{1/6}\sigma$  and  $\phi(r_m) = -\epsilon$ .  $\epsilon$  is usually referred to as the well depth. Thus, two parameters completely define the potential, with  $\sigma$  having units of distance and  $\epsilon$  having units of energy.

The Lennard-Jones potential is sometimes written in an equivalent form in terms of  $r_m$  instead of  $\sigma$

$$\phi(r) = \epsilon \left( \left( \frac{r_m}{r} \right)^{12} - 2 \left( \frac{r_m}{r} \right)^6 \right), \quad (5.7)$$

where, not surprisingly,  $\sigma = 2^{-1/6}r_m$ .

In this and later chapters it will be useful to express the Lennard-Jones potential in *scaled (or reduced) units*, in which the energy is expressed in units of  $\epsilon$  and distances in units of  $\sigma$ . The reduced variables are written as  $\phi^* = \phi/\epsilon$  and  $r^* = r/\sigma$ . With these definitions the Lennard-Jones potential becomes

$$\phi^*(r^*) = 4 \left( \left( \frac{1}{r^*} \right)^{12} - \left( \frac{1}{r^*} \right)^6 \right). \quad (5.8)$$

As we will discuss in detail in a discussion about molecular dynamics in Chapter 6, any calculation performed using the reduced potential  $\phi^*$  is valid, with the appropriate substitution of parameters, for any interaction described by the Lennard-Jones potential, i.e., the calculation can be performed in reduced units and the final energies are found by scaling by the appropriate  $\epsilon$  and the distances by the appropriate  $\sigma$ .

### Evaluating the Lennard-Jones model for gas-phase atoms

The prototypical systems described by the Lennard-Jones potential are the rare-gas atoms (He, Ar, . . .). They are closed-shell, so no bonding takes place, and their long-range interactions are dominated by van der Waals forces. Thus, if the Lennard-Jones model should work well for any material, it should be for these.

In Figure 5.4 we compare the experimental interatomic potential between two Ar atoms with the best fit of that potential to a Lennard-Jones potential. The experimental curve was determined in a molecular beam scattering experiment [16]. Comparison of the experimental curve with the Lennard-Jones potential shows that the Lennard-Jones potential is somewhat too stiff (i.e., the repulsive wall is too steep) and the well is a little too shallow. While the shape of the Lennard-Jones potential is reasonable, it is not overly accurate, which is not surprising given its simplicity and reliance on just two parameters. Also, as discussed in Section 5.2.1, the actual form of the short-range potential is best modeled with an exponential. The  $1/r^{12}$  form of the Lennard-Jones potential is not a particularly good representation of that form.

Table 5.1 Values of the Lennard-Jones parameters for the rare gases [32]

	Ne	Ar	Kr	Xe
$\epsilon$ (eV)	0.0031	0.0104	0.0140	0.0200
$\sigma$ (Å)	2.74	3.40	3.65	3.98

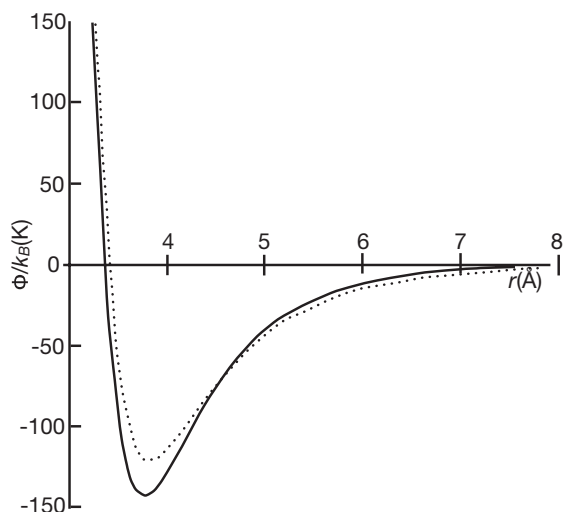


**Figure 5.4** Solid curve is the experimental Ar-Ar potential while the dashed curve is the best Lennard-Jones fit to that potential (adapted from [16]).

Based on scattering data (as well as other thermodynamic results), Lennard-Jones parameters have been determined for the interaction between like rare-gas atoms (i.e., He-He, Ar-Ar, . . .). These parameters are given in Table 5.1. The magnitude of the interactions is quite small, so we should not be surprised that solids consisting of these atoms are very weakly bound, showing, for example, very low melting points.

### Evaluating the Lennard-Jones model for solids

We can use the methods from Chapter 3 to calculate the zero K cohesive energy  $U$  for solids with interactions described by the Lennard-Jones potential. Using Eq. (3.7), for example, we could sum the interactions, truncating at some cutoff distance, as shown in Figure 3.3. The equilibrium structure at 0 K is that which gives the lowest cohesive energy. For example, in a material that has a cubic lattice structure, there is only one lattice constant,  $a$ . Its equilibrium value,  $a_o$ , corresponds to the minimum in the potential energy, i.e.,  $a_o$  is the value of  $a$  such that  $\partial U / \partial a = 0$ .

There is a class of systems, however, for which we do not need to do any summations at all; the sums have been evaluated by others and tabulated. Using special numerical methods, the lattice summation of potentials of the form  $1/r^n$  for  $n \geq 4$  has been performed for the basic perfect

**Table 5.2 Calculated and experimental properties of the rare gas solids.  
Parameters taken from [15]**

		Ne	Ar	Kr	Xe
$r_o$ (Å)	Experiment	3.13	3.75	3.99	4.33
	Theory	2.99	3.71	3.98	4.34
$u_o$ (eV/atom)	Experiment	-0.02	-0.08	-0.11	-0.17
	Theory	-0.027	-0.089	-0.120	-0.172
$B_o$ (GPa)	Experiment	1.1	2.7	3.5	3.6
	Theory	1.8	3.2	3.5	3.8

cubic structures: face-centered cubic (*fcc*), body-centered cubic (*bcc*), and simple cubic. No cutoffs were assumed, so these sums include all possible interactions.

In Appendix 5.11 we show how we can use the analytical sums to develop an *exact* form for the 0 K structure, cohesive energy, and bulk modulus,  $B = V(\partial^2 U / \partial V^2)$ , for systems described by any potential that is based only on terms of the form  $1/r^n$ , for example the Lennard-Jones potential. We emphasize that these sums are available only for the perfect cubic lattices and potentials of the form  $1/r^n$  for  $n \geq 4$ .

Using Eq. (5.40) and the potential parameters in Table 5.1, the zero-temperature cohesive properties of the rare-gas solids can be calculated based on the use of a Lennard-Jones potential. All of these materials form *fcc* solids at equilibrium, as do all systems described by a Lennard-Jones potential. In Table 5.2, we show the calculated equilibrium nearest-neighbor distance,  $r_o$ , the equilibrium cohesive energy per atom,  $u_o$ , and equilibrium bulk modulus,  $B_o$ , for a series of rare-gas solids. We compare those values with low-temperature experimental results in Table 5.2.<sup>8</sup> All in all, the simple Lennard-Jones potential (with parameters determined for gas-phase interactions) does a remarkably good job in describing the basic properties of rare-gas solids, with the largest errors for Ne, which, being a very light atom, has a large zero-point motion, which tends to lead to larger lattices.<sup>9</sup>

In Figure 5.5a we show the dependence of the cohesive energy per atom on the volume per atom in scaled units, in which we also identify the position and value of the energy minimum, corresponding to the equilibrium states of the system given in Eq. (5.40). Note that these two parameters only identify a single point on the cohesive energy curve. The bulk modulus, on the other hand, is a measure of the *shape* of the cohesive energy at the equilibrium point and, as such, is a much more informative measure of how well a potential describes the interactions.

The cohesive energy curve  $U(V)$  in Figure 5.5a was calculated at  $T = 0$  K, which makes the thermodynamics simple. For example, at constant temperature and volume, the free energy

<sup>8</sup> Please see Appendix A for a discussion of units, including GPa (=10<sup>9</sup> Pascals).

<sup>9</sup> Zero-point motion is described in Appendix F.5.2.

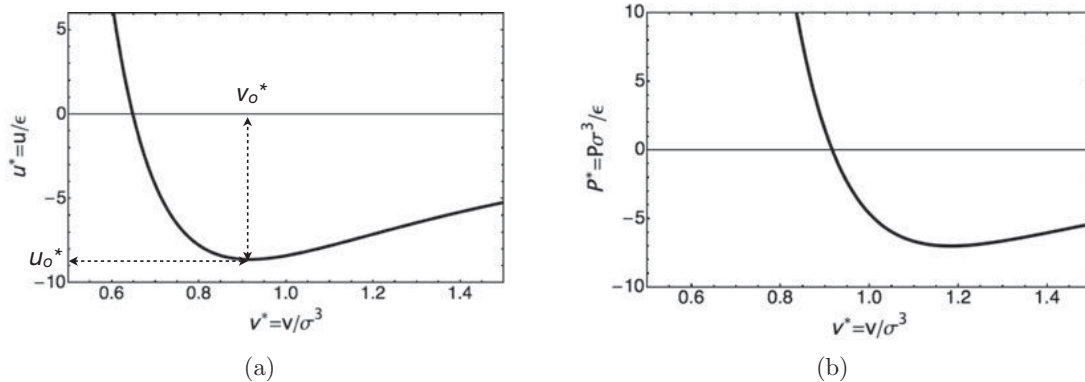


**Figure 5.5** (a) Cohesive energy per atom of the Lennard-Jones solid  $u^* = u/\epsilon$  as a function of the volume per atom  $v^* = v/\sigma^3$ , from Eq. (5.39).  $v_o^*$  and  $u_o^*$  are the equilibrium values from Eq. (5.40). The bulk modulus is proportional to the curvature of this curve at equilibrium. (b) The pressure for the Lennard-Jones solid at 0 K.

is the Helmholtz free energy  $A$  and the pressure is  $P = -(\partial A / \partial V)_{NT}$ . At 0 K,  $A = U$ , and so the pressure can be calculated from Figure 5.5a as  $P = -(\partial U / \partial V)_{NT}$ . Based on Eq. (5.39), in which the analytic form for the cohesive energy as a function of the volume is given, the pressure was calculated and plotted in Figure 5.5b. Note that  $P = 0$  at  $v^* = v_o^*$  as expected. Once we have the pressure, the Gibbs free energy is  $G = U + PV$  at 0 K.

From the agreement between experiment and calculations in Table 5.2, we see that the Lennard-Jones potential describes the shape of interactions between rare-gas atoms reasonably well, at least near equilibrium. The Lennard-Jones potential does much less well for systems under pressure, in which the nearest-neighbor atoms are forced up the repulsive wall of the potential. Moreover, the rare gas solids are not representative of most materials. The Lennard-Jones potential, while useful, does not describe the interactions between atoms in most materials very well at all, so other forms are needed if we want accurate calculations of the properties of materials.

### 5.3.2 The Mie potential

The Lennard-Jones potential has two parameters,  $\epsilon$  and  $\sigma$ , that can be adjusted to improve the comparison between calculated quantities and experiment. Table 5.2 shows comparison with three quantities. We could adjust the two parameters in the Lennard-Jones potential to match two of those quantities, for example  $r_o$ , which depends only on  $\sigma$ , and  $u_o$ , which depends only on  $\epsilon$ . With only two parameters, we cannot necessarily fit  $B_o$  as well.

Improvements can be made to the Lennard-Jones potential by adding additional parameters.<sup>10</sup> One approach would be to have the exponents in the  $1/r^{12}$  and  $1/r^6$  parts of the potential be adjustable parameters, i.e., instead of  $r^{-12}$ , perhaps  $r^{-11}$  would be a better description of the

<sup>10</sup> Adding parameters corresponds to the “iterate and improve” phase of Figure 1.2.

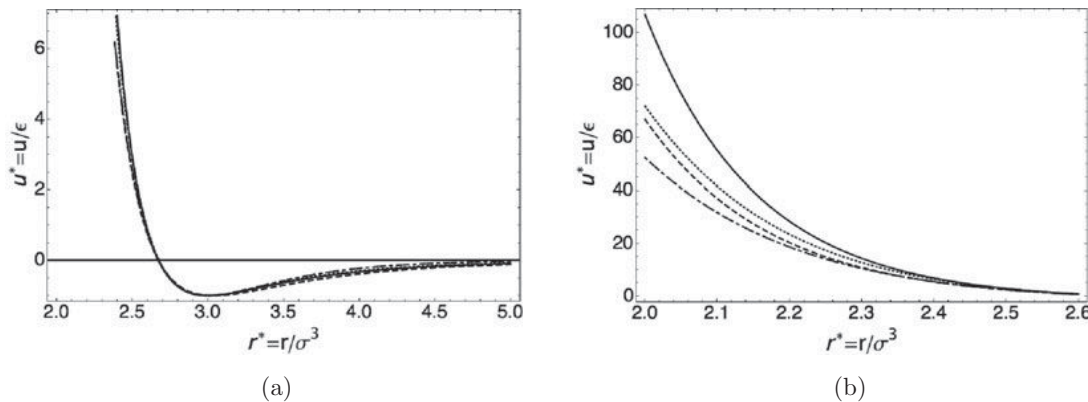


**Figure 5.6** Comparisons between pair potentials, all calculated with the potential minimum at  $r_m = 3$  and the Lennard-Jones  $\sigma = 2^{1/6}r_m$ . The well depth was  $\epsilon = 1$  for all cases. Shown are the Lennard-Jones potential (solid curve), the Mie potential with  $m = 10$  and  $n = 6$  (the long-dashed curve), the Morse potential with  $\alpha = 2.118$  (dot-dashed curve), and the Born-Mayer potential with  $\alpha = 4.88$  (dotted curve). (a) The well region. The potentials are all forced to have the same minimum and all go to zero at  $r = \sigma$ . (b) The short-range part of the potentials.

short-range interactions in some systems. A variation of the Lennard-Jones form, called the Mie potential (or the  $mn$  Lennard-Jones potential), takes this approach, replacing  $1/r^{12}$  with  $1/r^m$  and  $1/r^6$  with  $1/r^n$ . Writing the Mie potential as

$$\phi_{mn}(r) = \frac{\epsilon}{m-n} \left( \frac{m^m}{n^n} \right)^{\frac{1}{m-n}} \left( \left( \frac{\sigma}{r} \right)^m - \left( \frac{\sigma}{r} \right)^n \right) \quad (5.9)$$

yields an equivalent form to the Lennard-Jones potential. The Mie potential thus has four parameters:  $\sigma$ ,  $\epsilon$ ,  $m$ , and  $n$ . The parameters  $\sigma$  and  $\epsilon$  have the same meaning as in the standard Lennard-Jones potential:  $\phi_{mn}(\sigma) = 0$  and  $\phi_{mn}(r_m) = -\epsilon$ , where the minimum is located at

$$r_m = (m/n)^{1/(m-n)}\sigma. \quad (5.10)$$

If  $m = 12$  and  $n = 6$ , the standard Lennard-Jones potential is obtained.<sup>11</sup> The  $mn$  potential yields somewhat better results for some systems, especially those with repulsive potentials that are less steep than the  $1/r^{12}$  term in the standard Lennard-Jones potential. We compare the Mie potential with others in Figure 5.6.

The lattice sums in Appendix 5.11 of this chapter for cubic, body-centered cubic and face-centered cubic lattices are tabulated for any potentials of the form  $1/r^n$ . Thus, they are equally applicable to the Mie potentials as to the standard Lennard-Jones potential. For example, in Eq. (5.41) expressions are given for the equilibrium cohesive properties for systems described by the Mie potential.

<sup>11</sup> It is useful to rewrite the Mie potential in Eq. (5.9) in terms of  $r_m$  instead of  $\sigma$ . What is the relation between  $\sigma$  and  $r_m$ ?

### 5.3.3 Other pair potentials

The basic form of any pair interaction will be similar to that of the Lennard-Jones potential, with a short-range repulsion and an attractive well at long range. Like the Lennard-Jones form, these potentials best describe systems made up of closed-shell atoms, ions, and molecules. Here we describe two of the more commonly used forms.

The *Born-Mayer* potential, which is sometimes referred to as the exponential-6 (or *exp-6*) potential, is

$$\phi(r) = Ae^{-\alpha r} - \frac{C}{r^6}, \quad (5.11)$$

where  $A$ ,  $C$ , and  $\alpha$  are positive constants that depend on the identities of the interacting atoms.  $\alpha$ , with units of 1/length, governs the steepness of the repulsive wall. An advantage over the Lennard-Jones potential is that the exponential function that describes the repulsive part of the potential matches what we expect from the electronic distributions of the interacting atoms (Eq. (5.3)) and is thus more physically reasonable than the very repulsive  $1/r^{12}$  term in the Lennard-Jones potential. The long-range part of the potential is the van der Waals  $-1/r^6$  attraction. The Born-Mayer potential is often used for ionic systems, where the electrostatic interactions between the ions are included, as discussed in Section 5.4.

At times, it is convenient to write the *exp-6* potential as

$$\phi(r) = \frac{\epsilon}{\alpha r_m - 6} \left\{ 6e^{-\alpha(r-r_m)} - \alpha r_m \left( \frac{r_m}{r} \right)^6 \right\}, \quad (5.12)$$

where the position of the minimum is  $r_m$  and the well depth is  $\epsilon$ . The parameters in Eq. (5.11) are related to  $r_m$ ,  $\epsilon$  and  $\alpha$  through the relations  $A = 6\epsilon \exp(\alpha r_m)/(\alpha r_m - 6)$  and  $C = \alpha r_m^7 \epsilon / (\alpha r_m - 6)$ . Note that this form is restricted to values of  $r_m$  and  $\alpha$  such that  $\alpha r_m - 6 > 0$ .

Arising from a simple theory of diatomic bond potentials, the *Morse potential* takes the form

$$\phi(r) = \epsilon \left\{ e^{-2\alpha(r-r_m)} - 2e^{-\alpha(r-r_m)} \right\}, \quad (5.13)$$

where, as usual,  $r_m$  is the position of the minimum,  $\epsilon$  is the well depth, and  $\alpha$  governs the shape of the potential. The Morse potential has a very soft repulsive wall and is sometimes used to model interatomic interactions in metals. Note that the interaction at long range falls off much more quickly than the van der Waals energy of Eq. (5.4).

In Figure 5.6 we compare the basic pair potentials: the Lennard-Jones potential (Eq. (5.6)), the Mie potential with  $m = 10$  and  $n = 6$  (Eq. (5.9)), the Born-Mayer potential (Eq. (5.11)), and the Morse potential (Eq. (5.13)). In all cases, the minimum was set at  $r_m = 3$ , with the well depth  $\epsilon = 1$ . To make the comparison more clear, the  $\alpha$  parameters in both the Born-Mayer and Morse potentials were adjusted until the value of  $r$  for which  $\phi(r) = 0$  matched the  $\sigma$  value in the Lennard-Jones potential,  $\sigma = r_m/2^{1/6}$ .<sup>12</sup> Given the constraints placed on the potentials such that their minimum and  $\sigma$  values all agree, it is not surprising that in Figure 5.6a, which

<sup>12</sup> The relation of the  $\sigma$  value to  $r_m$  is slightly different for the Mie potential, being given by Eq. (5.10), where we find that  $\sigma = 0.88r_m$  for the 10-6 Mie potential, as opposed to  $0.89r_m$  for the Lennard-Jones potential.

focuses on the well region, we do not see significant differences between the potentials. The potentials are very different, however, at shorter ranges, as shown in Figure 5.6b. In order of “steepness”, from most steep to least, the potentials are: Lennard-Jones, the Born-Mayer potential, the Mie 10-6 potential, and the Morse potential. The shape of this part of the potential affects the curvature at the well (and, thus, properties such as the bulk modulus) as well as the high-pressure properties, in which the atoms are squeezed close together. In general, the Lennard-Jones potential is too stiff, so one of the others is likely to be more appropriate for most applications. How one chooses the form and the parameters is discussed in Section 5.9.<sup>13</sup>

### 5.3.4 Central-force potentials and the properties of solids

Interatomic potentials that are functions only on the distance between the pairs of atoms are referred to as *central-force potentials*. All the potentials in this section are of that form. There are limitations, however, to the kind of materials that can accurately be described by central-force potentials. For example, perfect crystals with a single component whose interactions are described by central-force potentials will always take on simple structures like face-centered cubic, body-centered cubic, etc. Thus, central-force potentials cannot be used to model pure systems with more complicated structures.

There is also experimental evidence that using a central-force potential cannot provide an adequate description of the elastic behavior of solids. For example, as discussed in Appendix H.4, any deviation from the Cauchy relation  $c_{12} = c_{44}$  for systems with symmetric lattice positions is a measure of the deviation from central-force interactions in the material.<sup>14</sup> One way to express that deviation is to consider the ratio of the elastic constants  $c_{12}/c_{44}$ , which should equal 1 for systems that interact only through central forces. In Table 5.3 we give experimental values for  $c_{12}/c_{44}$  for a number of materials.

From Table 5.3, we see that a material whose interactions are described with the Lennard-Jones potential satisfies the Cauchy relation, as expected. A simple rare-gas solid, argon, also shows very small deviations from  $c_{12}/c_{44} = 1$ , indicating that a central-force pair potential description should also be effective in describing the elastic properties. Of the other materials in Table 5.3, only for NaCl does the Cauchy relation hold, with large deviations for metals (with  $c_{12}/c_{44} > 1$ ) and for covalently bonded materials (with  $c_{12}/c_{44} < 1$ ).<sup>15</sup> Thus, to accurately model most materials will generally require more complex potentials than those described in this section.

<sup>13</sup> It may be useful for the reader to compare the basic forms of pair potentials, for example: (a) plot the Mie potential for a series of values of  $m$  with  $n = 6$ . Compare the repulsive part of the potential. Repeat for a series of values for  $n$  with  $m = 12$ . (b) Compare the Lennard-Jones potential (LJ) with the Born-Mayer potential in Eq. (5.12) for a series of values of  $\alpha$  (keeping  $r_m$  the same for both potentials). (c) Repeat using the Morse potential of Eq. (5.13).

<sup>14</sup>  $c_{12} = \lambda$  and  $c_{44} = \mu$  are elastic constants, as discussed in Appendix H.

<sup>15</sup> The relation  $c_{12}/c_{44} < 1$  for covalently bonded materials can be readily explained by a consideration of the bonding, as described in [334].

**Table 5.3 Comparison of values for  $c_{12}/c_{44}$  for a number of materials. The value from calculations on a Lennard-Jones (LJ) potential are from [267], the data for Ar is from [168], while all other data are from Appendix 1 of [147]**

Material	$c_{12}/c_{44}$
“LJ”	1.00
Ar	1.12
Mo	1.54
Cu	1.94
Au	4.71
NaCl	0.99
Si	0.77
MgO	0.53
diamond	0.16

## 5.4 IONIC MATERIALS

Ionic solids typically consist of closed-shell ions with little charge in the interstitial regions (Figure 5.2). The simplest approach to describe the interactions between two ions,  $i$  and  $j$ , in an ionic material is to start with a simple pair potential,  $\phi_{ij}$ , which could be any of the forms presented in this chapter. We add to that potential the electrostatic, or Coulomb, interaction between the two ions

$$k \frac{q_i q_j}{r_{ij}}, \quad (5.14)$$

where  $r_{ij}$  is the distance between the two ions and  $q_i$  and  $q_j$  are the charges on ion  $i$  and  $j$ , respectively.  $k$  is a parameter whose value depends on the units, as discussed in Appendix E.1.<sup>16</sup> The net cohesive energy is

$$U = \frac{1}{2} \sum_{i=1}^N \sum_{j=1}^N' \left( \phi_{ij}(r_{ij}) + k \frac{q_i q_j}{r_{ij}} \right). \quad (5.15)$$

The sum of the Coulomb terms in Eq. (5.15) involves long-ranged interactions and requires special methods, which are discussed in Section 3.6.

<sup>16</sup> A discussion of the units and form of the Coulomb potential is given in Appendix E.